A Hybrid Iterative Algorithm of Amplitude Weighting and Phase Gradient Descent for Generating Phase-Only Fourier Hologram

Min Fan[1], Jin Yang[1], Chengtao Du[2*], Jie Fang[2], Haibo Wang[1], Chenlu Li[1]

[1] School of Electronic and Electrical Engineering, Hefei Normal University, Hefei 230061, China
[2] Department of Electrical and photo Engineering, West Anhui University, Lu'an 237012, China

Corresponding Author Email: ctdu@wxc.edu.cn

ABSTRACT

Reconstruction of target images from phase-only hologram (POH) has the advantages of high diffraction efficiency and no conjugate terms. The Gerchberg-Saxton (GS) algorithm is a classical algorithm applied to recover the phase, but it most likely stagnantes after a few iterations. This paper proposes a hybrid iterative algorithm of Amplitude Weighting and Phase Gradient Descent (AW-PGD) to generate a higher-quality POH. Firstly, the quadratic phase is used as the initial phase, zero-pads the periphery of the target image, and then multiplies the two to form the complex amplitude as the iterative initial value. During iteration, the amplitude of the reconstructed image is constrained by an adaptive dynamic exponential term in the signal region to improve the reconstruction accuracy, the constraint in the non-signal region is relaxed to reduce the computational effort at the same time; and the phase gradient descent technology is used to increase the iteration step and speed up the convergence. Finally, the target image amplitude is reconstructed based on the generated POH. The numerical simulation results show that the algorithm does not have a significant increase in time cost with better reconstruction quality than the GS, Weighted GS (WGS) and Adaptive Weighted GS (AWGS) algorithm.

1. INTRODUCTION

Since the birth of holography more than 60 years ago [1], it has evolved from traditional laser holography to today's Computer-Generated Holograms (CGHs) [2, 3]. CGHs don't require special holographic recording materials, but instead use Spatial Light Modulators (SLMs) to load CGHs. SLMs are highly flexible and are widely used in beam shaping [4], holographic displays [5] and atom trapping [6]. Since the current mainstream commercial SLMs can only modulate either the amplitude or the phase of the light wave, but not both directly, only phase-only or amplitude-only hologram can be loaded on the SLM [7]. Phase-Only Hologram (POH) has a higher diffraction efficiency than Amplitude-Only Hologram (AOH) and doesn't produce conjugate images [8], making POH an effective method for reconstructing high quality holograms.

The POH is a non-convex problem derived from complex amplitude images and there is no unique exact solution. Only an optimal solution under certain conditions can be obtained, and the quality of the POH will constrain the quality of the reconstructed image [9, 10]. Currently, there are two typies algorithms for generate POH, one is the iterative algorithms and the other is non-iterative algorithms. Non-iterative algorithms include phase mask-like methods [11-14], where the target image is multiplied with a phase mask on the image plane and then the phase of the complex amplitude on hologram plane is taken to reconstruct the target image, where the quadratic mask method mentioned in the references [15, 16] can obtain a higher signal-to-noise ratio. Other non-iterative algorithms, such as the Sampled Phase-Only

Hologram algorithm [17] and the Complementary Phase-Only Hologram algorithm [18] are available for ensuring reconstruction quality still, they are computationally intensive and require a high-performance SLM. These non-iterative algorithms can obtain the desired POH in one step, but the quality of the reconstructed image is not as high.

Iterative algorithms propagate light wave over the hologram plane and the image plane by the Fourier Transform (FT) and Inversion Fourier Transform (IFT), optimizing the calculation results based on the measurable amplitude distribution in the two planes and the constraints imposed on the two planes to obtain the phase information of the light field in the hologram plane. The Gerchberg-Saxton (GS) [19] algorithm, proposed in 1972, is a classical iterative algorithm in the field of phase extraction and can achieve high-quality reconstructed images. But it suffers from the problem of falling into optimal local solution and slow convergence, i.e., increasing the number of iterations won't lead to better reconstruction quality. In addition, using a random phase as the initial phase causes unexpected interference between adjacent sampling points in the reconstructed image based on POH, resulting in uneven line and edge levels and speckle noise in the reconstructed image. Thus, iterative algorithms need to be optimized in suppressing speckle noise and improving reconstruction quality. In terms of suppressing speckle noise, improvements can be made in the initial phase setting, with non-random phases such as the quadratic phase and the conical phase used as the initial value of the phase iteration in some studies [20, 21]. To avoid the speckle noise caused by the random initial phase, in 2021 Chen et al. proposed an initial phase with bandwidth constraint, which ensures the bandwidth constraint

of the reproduced optical field and distributes the whole signal energy as evenly as possible to the hologram region [22]. Pang et al. proposed to use the quadratic phase as the initial phase, and was able to determine the relevant parameters of the quadratic phase according to the imaging and geometric relationships of the lens, thus significantly improving the scattering noise, but there are optical artifacts in the reconstructed image [23]. In the same year, Wu Y. proposed an approximate phase, using a set of plane waves with discrete orientations to represent the approximate quadratic phase, which can effectively suppress the appearance of speckle noise and artefacts [24]. In terms of improving the reconstruction quality and convergence speed, constraints need to be continuously optimised. For example, Fienup proposed to improve the convergence speed by introducing a difference between the target image and the computed image in 1982, but the noise suppression parameters need to be manually controlled [25]. To better tackle this problem, the Weighting GS (WGS) algorithm for kinoform implemented with POH was proposed by Alexander Kuzmenko in 2011, where the computed amplitude is multiplied by the weighting coefficients in each iteration to improve convergence [26]. But this method suffers from feedback instability. To solve this problem, reference [24] proposed the Adaptive Weighted GS (AWGS) algorithm with a flexible setting of amplitude constraints, which optimizes the weighting coefficients from the structure of proportional terms to the exponential terms to avoid feedback instability. In contrast to the previous approaches which is imposing amplitude constraints on the whole target image, some scholars have adopted the approach of dividing the target image into signal and non-signal regions, where different amplitude constraint strategies are adopted in the different regions in order to improve the reconstruction quality [27-28]. In addition to the above amplitude constraint-based algorithms, scholars have also proposed methods to constrain the phase as well. For example, in 2017, Wang combined gradient descent and weighting techniques with GS algorithm and applied them to Diffractive Optical Element (DOE) and CGH to demonstrate the effectiveness of this method [29]. Another example is Double-Constraint GS (DBGS) algorithm, which suppresses speckle noise [30]. This algorithm constrains the amplitude and phase in the signal region only. However, these algorithms still suffer from insufficient reconstruction accuracy. Therefore, the methods need to be optimized for higher reconstruction quality without increasing the complexity of the optical path system.

This paper proposes a hybrid constrained iterative algorithm for generating POH. In this algorithm, zero-pads the periphery of the target image, which is thus divided into signal and non-signal regions, and multiplied with the quadratic phase to form the initial complex amplitude. An exponential amplitude constraint is applied on the reconstructed image to improve the reconstruction accuracy, and a gradient descent technology is used on the phase of hologram to accelerate the convergence speed. Numerical experimental results show that the algorithm proposed in this paper can effectively accelerate the convergence and improve the quality of the reconstructed images.

2. KNOWLEDGE CONTEXT

This paper presents an optimization algorithm based on the GS algorithm, whose calculated POH can be loaded into the

SLM in the Fourier hologram projection system to realize hologram projection. Here is an introduction to the principle of Fourier hologram projection and the GS algorithm.

2.1 Principle of Fourier hologram projection

The principle of Fourier hologram projection is shown in Figure 1. The hologram plane is placed on the front focal plane of the Fourier lens, and the image plane is on the back focal plane. The SLM of the hologram plane is loaded the POH firstly, which is carrying all the information of the target image. The plane light is incident vertically onto the hologram plane and modulated by the SLM. The light then passes through the Fourier lens for FT. The intensity distribution of the target image is displayed on the image plane of the back focal plane of the lens.
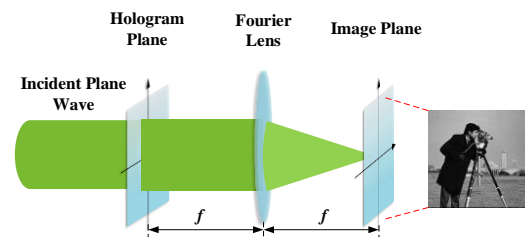

Figure 1. Schematic for Fourier hologram projection system

### 2.2 Principle of generating POH based on GS method

The GS algorithm is a classical iterative phase retrieval algorithm. Figure 2 presents its fundamental principle. The steps are as follows: 1) Assume μ_0 as the initial phase value and form the initial complex amplitude $u_0 = 1 \cdot exp(j\mu_0)$ into the iteration; 2) Propagate it through FT to the image plane to obtain U_1; 3) Replace its amplitude with the target image amplitude $|A_{target}|$ to obtain U_1'; 4) Propagate U_1' to the hologram plane through IFT to obtain u_1'; 5) Replace the amplitude of u_1' by 1 as the initial value for the next iteration. Repeat steps 2-5 until the quality of the reconstructed image meets the requirements, where u_k is the complex amplitude of the hologram after k iterations, its phase is POH, and the amplitude of U_k is the reconstructed image amplitude.

Although the GS algorithm can generate higher quality POH, it still suffers from slow convergence, falling into local minima, insufficient reconstruction accuracy and feedback instability. Many scholars have studied many improved algorithms based on the GS algorithm, such as the WGS algorithm and the AWGS method. Figure 3 shows a comparison of the Root Mean Squared Error (RMSE) curves of the GS, WGS and AWGS algorithm, in which the horizontal coordinate is the number of iterations and the vertical coordinate is the value of RMSE. It can be seen that the WGS algorithm suffers from instability, and AWGS algorithm converges faster and has better reconstruction quality than GS algorithm.

The three methods are all based on amplitude constraints. There is still room to improve the reconstruction quality. If the generated phase is also constrained on the hologram plane, it will lead to better reconstruction quality. In this paper, we combine amplitude weighting strategy and gradient descent technology to propose an Amplitude Weighting and Phase Gradient Descent (AW-PGD) hybrid algorithm.
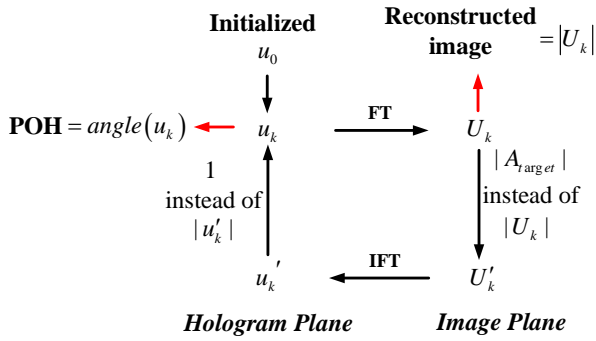
**Figure 2.** Principle of generating POH based on GS algorithm
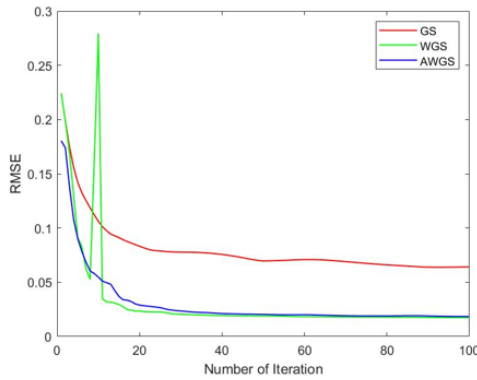
**Figure 3.** Comparison of RMSE of GS, WGS and AWGS algorithm

3. HYBRID METHOD OF AW-PGD

The proposed AW-PGD hybrid algorithm consists of two parts. In the first part, zero-padding is applied around the target image to improve the reconstruction quality. The black frame formed by zero-padding is called the non-signal region, and the target image region inside the black frame is called the signal region. The image after zero-padding is called the target image, as shown in Figure 4. The purpose of zero-padding is to move the background noise from the signal region to the non-signal region for a high Signal-to-Noise Ratio (SNR) in the reconstructed image [31].

The second part is the hybrid constraint iteration. The hybrid constraint reflects two aspects. One is the feedback constraint of the exponential term is applied on the magnitude of the reconstructed image on the image plane to improve the reconstruction accuracy. The other is the phase of hologram is constrainted by gradient descent technology to increase the iteration step to speed up the convergence. Figure 5 presents the block diagram of the algorithm.
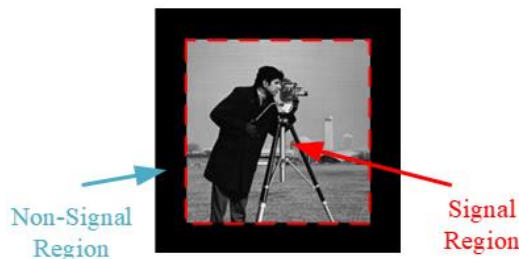
Figure 4. The image is divided into signal region and non-signal region by zero-padding
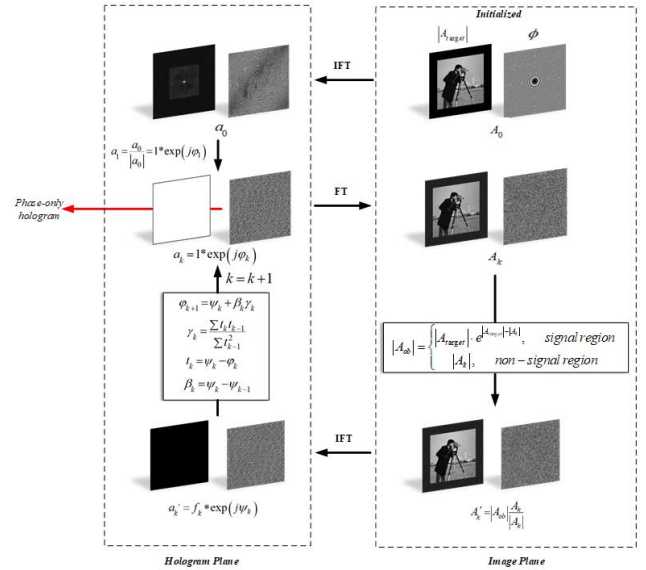
Figure 5. Scheme of amplitude weighting and phase gradient descent (AW-PGD) hybrid algorithm

A_0 is the initial complex amplitude of the image plane, which can be expressed as follows:

$$A_0 = \left| A_{t\,arg\,et} \right| \cdot \exp\left(j\phi \right) \tag{1}$$

where, $\left| A_{t\,arg\,et} \right|$ is the intensity of the target image containing the zero-padding region. Since multiplying the target image with a quadratic phase mask has the effect of removing some of the speckle noise, ϕ takes the quadratic phase, the expression of which is given as Eq. (2):

$$\phi = am^2 + bn^2 \tag{2}$$

here, m and n are the coordinates of the signal region; a and b are the parameters between 0 and 1. According to reference [32], a and b can take the values:

$$a \approx \frac{\pi}{M} \tag{3}$$

$$b \approx \frac{\pi}{N} \tag{4}$$

M and N are the numbers of horizontal and vertical pixel points in the signal region respectively.

a_0 is the complex amplitude of A_0 propagated to the hologram plane after IFT. Only the phase of a_0 is taken to obtain a_1, starts the iterative process. k denotes the number of iterations, and k starts from $k=1$. The iterative process is as follows:

Step 1: a_k represents the complex amplitude of hologram of k-th iteration, which phase distribution is φ_k. a_k is propagated through FT to the image plane to obtain the complex amplitude A_k.

Step 2: Replace the amplitude of A_k with $|A_{ob}|$ to become A'_k.

Step 3: A'_k is propagated back to the hologram plane via IFT to obtain the complex amplitude $a_k{'}$, ψ_k is the phase

distribution of $a_k{'}$, and ψ_k becomes φ_{k+1} after a gradient descent to the next iteration.

The amplitude of A_k is the reconstructed image and the phase of a_k is the desired POH. Repeat the above steps until the quality of the reconstructed image or the number of iterations meets the requirements.

In the above iterative process, the amplitude constraint of A_k on the image plane is

$$\left|A_{ob}\right| = \begin{cases} \left|A_{t\,\mathrm{arget}}\right| \cdot e^{\left|A_{t\,\mathrm{arget}}\right| - \left|A_k\right|}, & signal \quad region \\ \left|A_k\right|, & non-signal \quad region \end{cases} \tag{5}$$

This gives the complex amplitude of the image plane after the amplitude constraint $A_k{'}$:

$$A_k' = \left|A_{ob}\right| \frac{A_k}{\left|A_k\right|} \tag{6}$$

After IFT of $A_k{'}$, we got $a_k{'} = f_k * exp(j\psi_k)$, where, f_k is the amplitude of the hologram in the $k-th$ iteration and ψ_k is the phase of the hologram before gradient descent in the $k-th$ iteration, using the gradient descent technology to act with the phase for faster convergence. The phase φ_{k+1} after gradient descent is defined as Eq. (7):

$$\varphi_{k+1} = \psi_k + \beta_k \gamma_k \tag{7}$$

where, β_k is the direction of the gradient, defined as the difference between ψ_k and ψ_{k-1}, ψ_{k-1} is the the phase of the hologram before gradient descent in previous iteration:

$$\beta_k = \psi_k - \psi_{k-1} \tag{8}$$

γ_k is the acceleration factor:

$$\gamma_k = \frac{\sum t_k t_{k-1}}{\sum t_{k-1}^2} \tag{9}$$

where, the expression for t_k is as Eq. (10):

$$t_k = \psi_k - \varphi_k \tag{10}$$

thus constitutes an iterative add-on $\beta_k \gamma_k$, increasing the gradient step size of the phase to speed up convergence.

4. EXPERIMENTAL VERIFICATION AND ANALYSIS

To verify the effectiveness of the algorithm proposed in this paper, we carried out numerical simulations and compared with the quadratic-phase-based GS, WGS and AWGS algorithms. Here, we applied some evaluation functions to compare the experimental results quantitatively. The first evaluation function is the RMSE between the reconstructed image and the target image, which is defined as follows:

$$RMSE = \sqrt{\frac{1}{MN}\sum_{m=1}^{M}\sum_{n=1}^{N}\left[A_k(m,n) - A_{t\,\mathrm{arget}}(m,n)\right]^2} \tag{11}$$

where, M and N are the numbers of horizontal and vertical pixel points in the signal region image, $A_k(m,n)$ is the intensity distribution of the reconstructed image of $k-th$ iteration, and $A_{t\,arget}(m,n)$ is the intensity distribution of the target image. The RMSE is a number greater than or equal to zero, with smaller values indicating better reconstruction quality.

The second evaluation function is Structural Similarity (SSIM), which is defined as:

$$SSIM = \frac{\left(2\mu_{t\,\mathrm{arger}}\mu_k + c_1\right)\cdot\left(2\sigma_{t\,\mathrm{arget},k} + c_2\right)}{\left(\mu_{t\,\mathrm{arget}}^2 + \mu_k^2 + c_1\right)\cdot\left(\sigma_{t\,\mathrm{arget}}^2 + \sigma_k^2 + c_2\right)} \tag{12}$$

where, $\mu_{t\,arger}$ and μ_k are the mean of the target image and the reconstructed image respectively; $\sigma_{t\,arget}$ and σ_k are the standard deviation of the two respectively; $\sigma_{t\,arget,k}$ is the covariance between the two; and c_1 and c_1 are tiny numbers to avoid the denominator being zero. SSIM takes values between 0 and 1, with larger values representing better reconstruction.

The third evaluation function is the Peak Signal-to-Noise Ratio (PSNR), which is defined for 8-bit greyscale images as:

$$PSNR = 20\log\left[\frac{255}{RMSE}\right] \tag{13}$$

The higher the value, the better the reconstruction.

In this simulation experiment, the target image selected is 'cameraman'. The resolution of both the target image and the hologram plane after zero-padding is taken as 512×512 pixels, the size of the signal area is 300×300 pixels, and the pixel size is $12\mu m$. See Figure 6(a). According to Eq. (3) and Eq. (4), the parameters of the quadratic phase a and b are both set to 0.01, as shown in Figure 6(b).

(a) Target image   (b) Quadratic initial phase
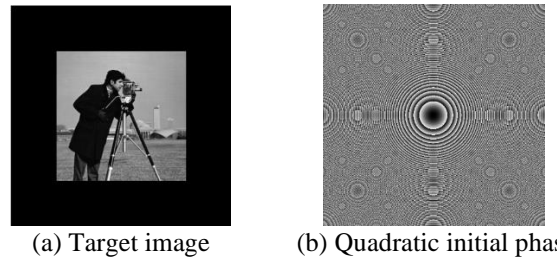
Figure 6. Target image 'cameraman' and initial quadratic phase

Figure 7 presents the POHs and reconstructed images generated by the GS, WGS, AWGS and AW-PGD GS algorithms at different numbers of iterations, as well as the values of the three evaluation parameters foreach reconstructed image. It shows that the reconstruction quality based on these four algorithms generally improves as the number of iterations increases. The RMSE of the GS algorithm is 0.073 at 50 iterations and drops to 0.0635 at 300 iterations, indicating that the reconstruction quality does not increase significantly with the number of iterations and falls into the trap of a locally optimal solution. The quality of the reconstructed images doesn't become better when the number of iterations increases. Instead, the quality decreases. The AWGS algorithm is better than the GS and WGS algorithms. Although the reconstruction quality using the AW-PGD

algorithm is average at a low number of iterations, the reconstruction quality is better than the other three algorithms as the number of iterations increases, with the RMSE value

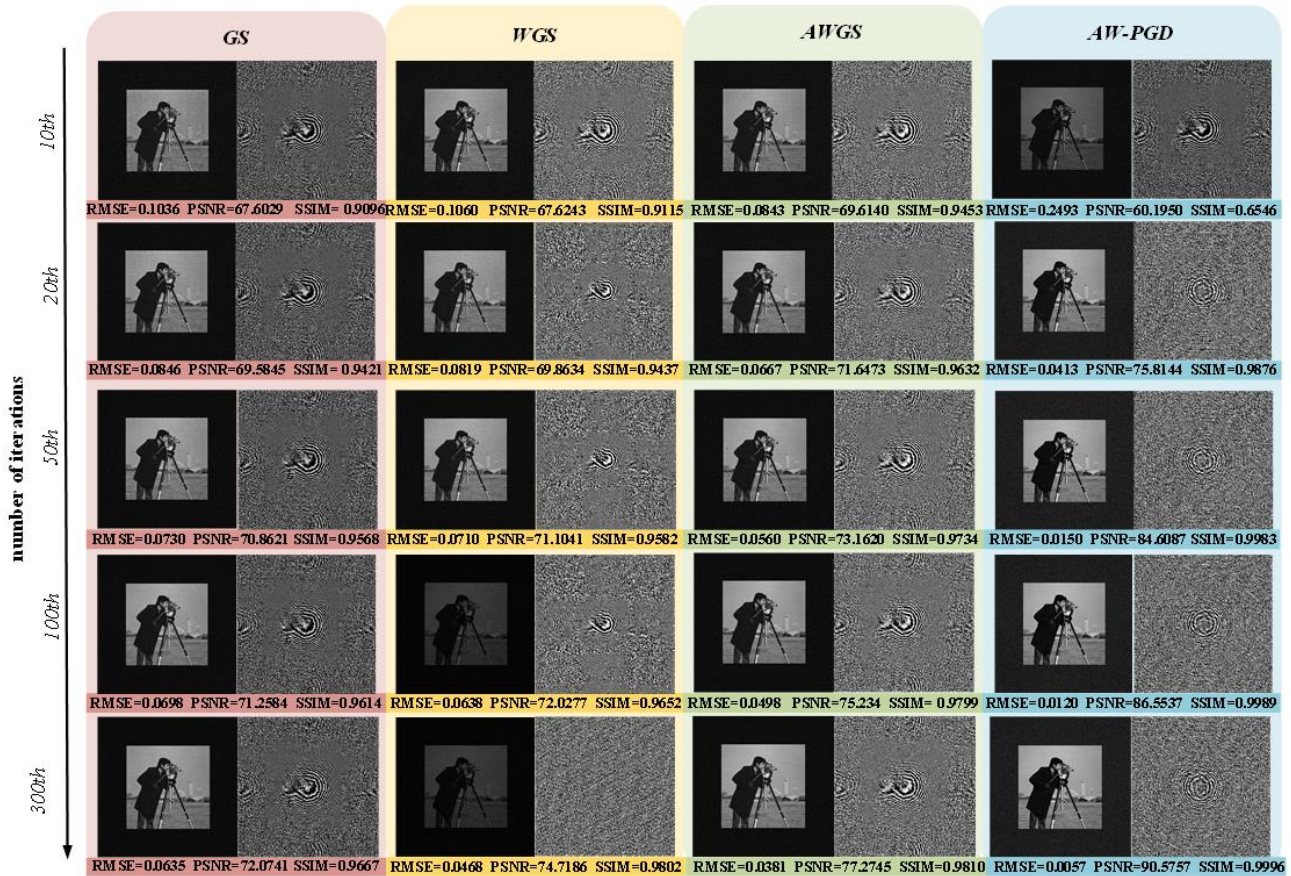down to 0.0057 at 300 iterations. The SSIM and PSNR also indicate the superiority of the AW-PGD algorithm.

Figure 7. Reconstructed image and POHs under different numbers of iterations by different algorithm
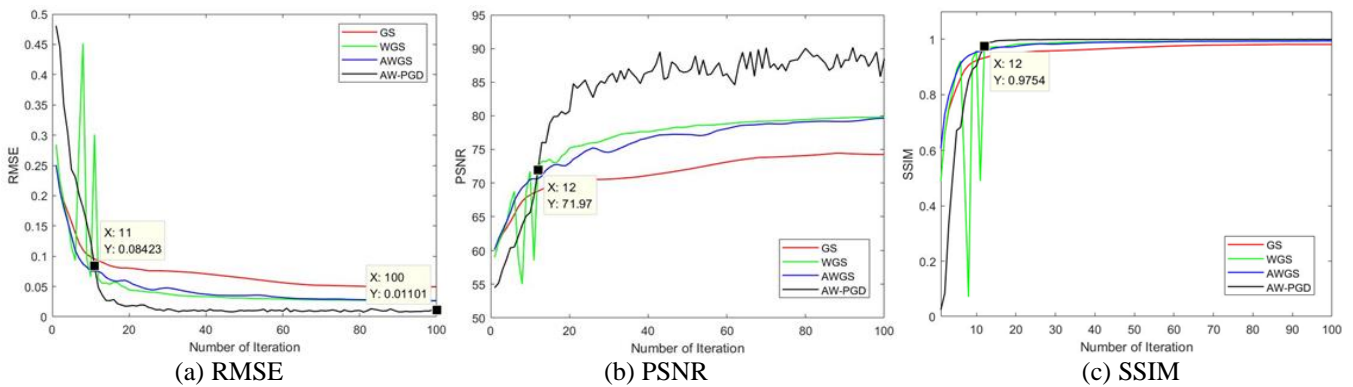

(a) RMSE   (b) PSNR   (c) SSIM

Figure 8. Comparison of reconstructed quality parameter

To see more clearly the relationship between the number of iterations and reconstruction quality, Figure 8 compares the values of the three parameters under the four algorithms. Figure 8(a) shows the RMSE under different number of iterations. It shows that although the AW-PGD algorithm is not the best when the number of iterations is small, the RMSE of the AW-PGD algorithm starts to perform better than the remaining three algorithms after 11 iterations, with an RMSE value of 0.08423. At the 100th iteration, the RMSE drops to 0.01101, which is much better than the remaining three algorithms. Figure 8(b) shows the SSIM curve and Figure 8(c) shows the PSNR value curve. Both parameter curves show the superiority of the AW-PGD algorithm.

To verify the effectiveness of the method proposed in this paper for other images, we used 'Lena', 'Lifting body' and 'Baboon' as the target images for a simulation experiment. The reconstructed images based on these four algorithms are compared under the same parameters setting. In this experiment, the number of iterations was 100 and the rest of the parameters were set as above. In Figure 9, (a), (b), (c) and (d) present the reconstructed results and POHs obtained based on the GS, WGS, AWGS and AW-PGD algorithms respectively, with the values of RMSE, PSNR and SSIM compared to the target image marked below each reconstructed image. It can be seen that the AW-PGD

algorithm also delivers better results than the other three algorithms when used for other target images.

We also compared the time cost of the AW-PGD algorithm with the other three algorithms, as shown in Table 1. Since above we found that the algorithm converges at around ten iterations, we also wanted to investigate further whether the time cost increases when the number of iterations is increase compared to the other three algorithms. Therefore, the number of iterations was set to 20, 50 and 100, and the rest of the parameters were the same as above. It can be seen that at 20 iterations, the time cost of the AW-PGD algorithm is similar to that of the AWGS algorithm; at 100 iterations, the AW-PGD algorithm increases the time cost by less than 1s.

Table 1. Comparison of time cost of the four algorithms under different number of iterations

	20	50	100
GS	1.486s	2.101s	3.151s
WGS	1.560s	2.370s	3.830s
AWGS	1.814s	2.596s	3.693s
AW-PGD	1.816s	2.700s	4.490s

In the AW-PGD method, the amplitude of the target image is divided into signal and non-signal regions, hence it is necessary to investigate the effect of the selection of the signal region size on the reconstruction effect and the time cost.
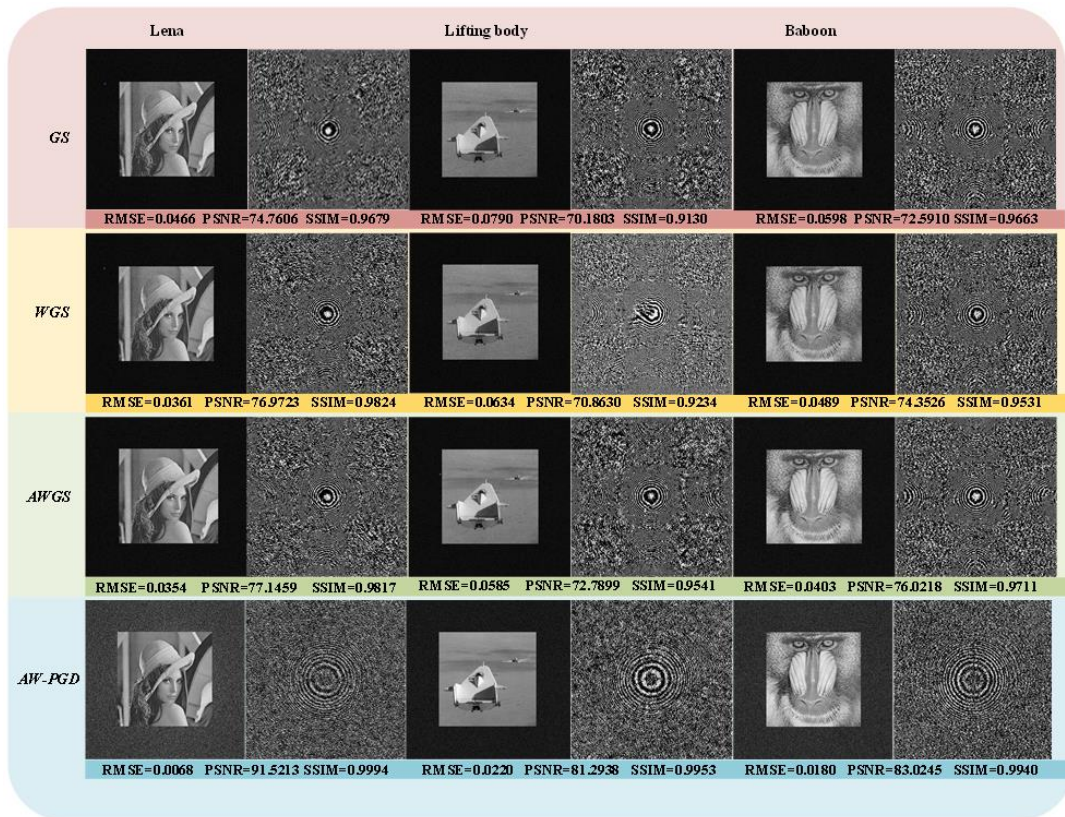
Figure 9. Reconstruction of different target amplitude from POH based on GS, WGS, AWGS and AW-PGD
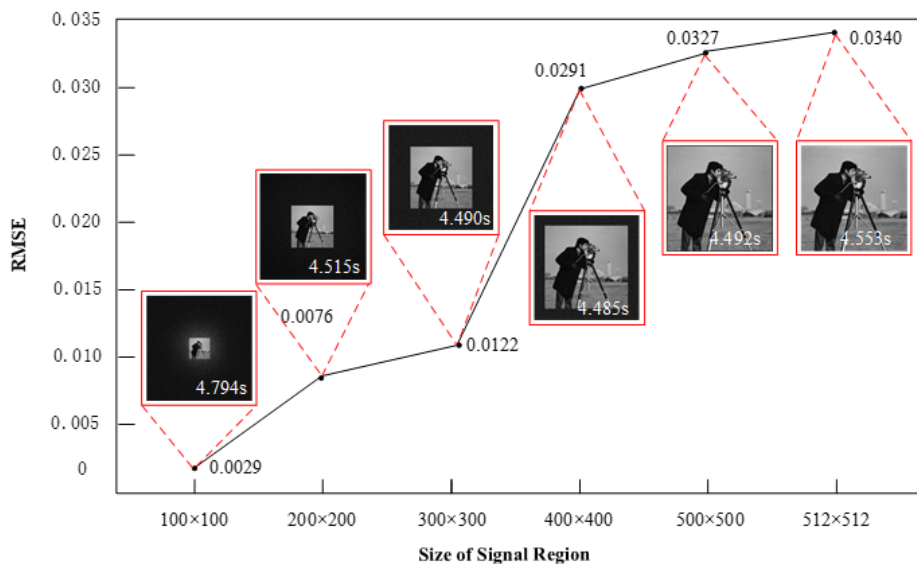
Figure 10. The relationship between the size of the signal region and RMSE and time cost

Figure 10 illustrates the relationship between the signal region size and the RMSE value and time cost. Here, the size of the entire target image, including the non-signal region, is 512×512 pixels, where the size of the signal region is 100×100, 200×200, 300×300, 400×400, 500×500 and 512×512. The corresponding parameters of the quadratic phase are selected as 0.03, 0.01, 0.007, 0.006 and 0.0061, with 100 iterations. It can be seen that as the signal area increases, the RMSE values increase and the reconstruction quality decreases, with little effect on the time cost.

5. CONCLUSIONS

This paper proposes a hybrid constrained AW-PGD iterative algorithm to compute and generate higher quality POHs. Use the quadratic phase as the initial phase because the quadratic phase has the advantage of suppressing speckle noise. By the way of zero-padding around the target image to improve the reconstruction quality. In the process of iteration, an adaptive dynamic constraint strategy is used on the image plane to improve the reconstruction quality and relax the constraint on the non-signal region to reduce the computational effort; a gradient descent algorithm is used on the hologram plane to speed up the convergence. Numerical simulation results show that this method has higher reconstruction quality than the GS, WGS and AWGS algorithms, and does not significantly increase the time cost. In addition, this paper investigates the effect of the selection of the signal region size on the reconstruction effect and time cost. The algorithm has the advantages of low computational effort, high reconstruction quality and simple optical path. Accordingly, the algorithm has good prospects for applications in hologram projection and atom capture.

REFERENCES

[1] Gabor D. (1948). A new microscopic principle. Nature, 161(4089): 777-778. https://doi.org/10.1038/161777a0

[2] Blinder, D., Schelkens, P. (2020). Phase added sub-stereograms for accelerating computer-generated holography. Optics Express, 28(11): 16924-16934. https://doi.org /10.1364/OE.388881

[3] Wang, Z., Zhu, L.M., Zhang, X., Dai, P., Lv, G.Q., Feng, Q.B., Wang, A.T., Ming, H. (2020). Computer-generated photorealistic hologram using ray-wavefront conversion based on the additive compressive light field approach. Optics Letters, 45(3): 615-618. https://doi.org/10.1364/OL.383508

[4] Pang, H., Liu, W., Cao, A., Deng, Q. (2019). Speckle-reduced holographic beam shaping with modified Gerchberg–Saxton algorithm. Optics Communications, 433: 44-51. https://doi.org/10.1016/j.optcom.2018.09.076

[5] Wang, W., Wang, X., Xu, B., Chen, J. (2021). Optical image encryption and authentication using phase-only computer-generated hologram. Optics and Lasers in Engineering, 146: 106722. https://doi.org/10.1016/J.OPTLASENG.2021.106722

[6] Kim, H., Kim, M., Lee, W., Ahn, J. (2019). Gerchberg-Saxton algorithm for fast and efficient atom rearrangement in optical tweezer traps. Optics express, 27(3): 2184-2196. https://doi.org/10.1364/OE.27.002184

[7] Li, B., Wang, J., Chen, C., Li, Y., Yang, R., Chen, N. (2020). Spherical self-diffraction for speckle suppression of a spherical phase-only hologram. Optics Express, 28(21): 31373-31385. https://doi.org/10.1364/OE.401679

[8] Hong, J., Li, J., Chu, D. (2022). Efficient dynamic control method of light polarization using single phase-only liquid crystal on silicon spatial light modulators for optical data storage. Applied Optics, 61(5): B34-B42. https://doi.org/10.1364/AO.443205

[9] Zheng, H., Zhou, C., Shui, X., Yu, Y. (2022). Computer-generated full-color phase-only hologram using a multiplane iterative algorithm with dynamic compensation. Applied Optics, 61(5): B262-B270. https://doi.org/10.1364/AO.444756

[10] He, Z., Sui, X., Jin, G., Chu, D., Cao, L. (2021). Optimal quantization for amplitude and phase in computer-generated holography. Optics Express, 29(1): 119-133. https://doi.org/10.1364/OE.414160

[11] Burckhardt, C.B. (1970). Use of a random phase mask for the recording of Fourier transform holograms of data masks. Applied Optics, 9(3): 695-700. https://doi.org/10.1364/AO.9.000695

[12] Zhao, T., Liu, J., Duan, J., Li, X., Wang, Y. (2019). Image quality enhancement via gradient-limited random phase addition in holographic display. Optics Communications, 442: 84-89. https://doi.org/10.1016/j.optcom.2019.02.026

[13] He, Z., Sui, X., Zhang, H., Jin, G., Cao, L. (2021). Frequency-based optimized random phase for computer-generated holographic display. Applied Optics, 60(4): A145-A154. https://doi.org/10.1364/AO.404934

[14] Tsang, P.W.M., Chow, Y.T., Poon, T.C. (2017). Generation of patterned-phase-only holograms (PPOHs). Optics Express, 25(8): 9088-9093. https://doi.org/10.1364/OE.25.009088

[15] Zea, A.V., Ramirez, J.F.B., Torroba, R. (2018). Optimized random phase only holograms. Optics Letters, 43(4): 731-734. https://doi.org/10.1364/OL.43.000731

[16] Shen, C., Qi, Y., Lv, S., Wang, B., Wei, S. (2022). Generation of non-iterative phase-only hologram based on a hybrid phase mask. Applied Optics, 61(6): 1507-1515. https://doi.org/10.1364/AO.449555

[17] Tsang, P.W.M., Chow, Y.T., Poon, T.C. (2015). Enhancement on the generation of sampled phase-only

holograms. Chinese Optics Letters, 13(6): 060901-060901. https://doi.org/10.3788/COL201513.060901

[18] Tsang, P.W.M., Chow, Y.T., Poon, T.C. (2016). Generation of complementary sampled phase-only holograms. Optics Express, 24(20): 23390-23395. https://doi.org/10.1364/OE.24.023390

[19] Gerchberg, R.W. (1972). A practical algorithm for the determination of plane from image and diffraction pictures. Optik, 35(2): 237-246.

[20] Shen, C., Qi, Y., Sun, J., Lv, S., Wei, S. (2021). Optimized iterative method for generating phase-only Fourier hologram based on quadratic phase. Optics Communications, 500: 127313. https://doi.org/10.1016/J.OPTCOM.2021.127313

[21] Pasienski, M., DeMarco, B. (2008). A high-accuracy algorithm for designing arbitrary holographic atom traps. Optics Express, 16(3): 2176-2190. https://doi.org/10.1364/OE.16.002176

[22] Chen, L., Tian, S., Zhang, H., Cao, L., Jin, G. (2021). Phase hologram optimization with bandwidth constraint strategy for speckle-free optical reconstruction. Optics Express, 29(8): 11645-11663. https://doi.org/10.1364/OE.422115

[23] Pang, H., Wang, J., Cao, A., Deng, Q. (2016). High-accuracy method for holographic image projection with suppressed speckle noise. Optics Express, 24(20): 22766-22776. https://doi.org/10.1364/OE.24.022766

[24] Wu, Y., Wang, J., Chen, C., Liu, C.J., Jin, F.M., Chen, N. (2021). Adaptive weighted Gerchberg-Saxton algorithm for generation of phase-only hologram with artifacts suppression. Optics Express, 29(2): 1412-1427. https://doi.org/10.1364/OE.413723

[25] Fienup, J.R. (2013). Phase retrieval algorithms: a personal tour. Applied Optics, 52(1): 45-56. https://doi.org/10.1364/AO.52.000045

[26] Kuzmenko, A., Iezhov, P., Kim, J.T. (2011). Weighting iterative Fourier transform algorithm for kinoform implemented with phase-only SLM. In Digital Holography and Three-Dimensional Imaging Optica Publishing Group.

[27] Chen, L., Zhang, H., He, Z., Wang, X., Cao, L., Jin, G. (2020). Weighted constraint iterative algorithm for phase hologram generation. Applied Sciences, 10(10): 3652. https://doi.org/10.3390/app10103652

[28] Alsaka, D.Y., Arpali, Ç., Arpali, S.A. (2018). A comparison of iterative Fourier transform algorithms for image quality estimation. Optical Review, 25(5): 625-637. https://doi.org/10.1007/s10043-018-0456-x

[29] Wang, H., Yue, W., Song, Q., Liu, J., Situ, G. (2017). A hybrid Gerchberg–Saxton-like algorithm for DOE and CGH calculation. Optics and Lasers in Engineering, 89: 109-115. https://doi.org/10.1016/j.optlaseng.2016.04.005

[30] Chang, C., Xia, J., Yang, L., Lei, W., Yang, Z., Chen, J. (2015). Speckle-suppressed phase-only holographic three-dimensional display based on double-constraint Gerchberg–Saxton algorithm. Applied Optics, 54(23): 6994-7001. https://doi.org/10.1364/AO.54.006994

[31] Zhai, T., Song, Q., Liao, E., Tam, A.M.W., Zhu, J. (2018). An approach for holographic projection with higher image quality and fast convergence rate. Optik, 159: 211-221. https://doi.org/10.1016/j.ijleo.2018.01.055

[32] Chen, L., Zhang, H., Cao, L., Jin, G. (2020). Non-iterative phase hologram generation with optimized phase modulation. Optics Express, 28(8): 11380-11392. https://doi.org/10.1364/OE.391518

NOMENCLATURE

u_0	the initial complex amplitude of the hologram plane in GS
U_1	the complex amplitude of FT of u_0
$\lvert A_{target} \rvert$	amplitude of target image
U_1'	complex amplitude of U_1 after amplitude replacement
u_1'	Inverse Fourier Transform of U_1'
u_k	complex amplitude of the hologram plane after k iterations in GS
U_k	complex amplitude of the image plane after k iterations in GS
A_0	the initial complex amplitude of the image plane in AW-PGD
a_0	IFT of A_0
a_1	the phase of a_0
a_k	the complex amplitude of the k-th iteration of the hologram plane
φ_k	the phase of a_k
A_k	the complex amplitude of the k-th iteration of the plane
$\lvert A_{ob} \rvert$	the amplitude of A_k'
A_k'	complex amplitude after the amplitude of A_k is replaced
a_k'	IFT of A_k'
f_k	the amplitude of the hologram plane in the k-th iteration
t_k	$\psi_k - \varphi_k$

Greek symbols

μ_0	initial phase in GS
ϕ	quadratic phase
ψ_k	the phase distribution of a_k'
φ_{k+1}	phase value of ψ_k after gradient descent
β_k	the direction of the gradient in the k-th iteration
γ_k	the acceleration factor in the k-th iteration

Subscripts

k	number of iteration
m	horizontal coordinates of signal area
n	vertical coordinates of signal area
a	the parameters between 0 and 1
b	the parameters between 0 and 1
M	horizontal pixel points in the signal area
N	vertical pixel points in the signal area
$RMSE$	root mean squared error
$PNSR$	peak signal noise ratio
$SSIM$	structural similarity